Effect of Volume Fraction and Particle Size on Wall Slip in Flow of Polymeric Suspensions

Sergul Acikalin Gulmus, Ulku Yilmazer

Department of Chemical Engineering, Middle East Technical University, Ankara, 06531, Turkey

Received 13 January 2005; accepted 18 March 2005
DOI 10.1002/app.21928
Published online in Wiley InterScience (www.interscience.wiley.com).

ABSTRACT: For especially highly concentrated suspensions, slip at the wall is the controlling phenomenon of their rheological behavior. Upon correction for slip at the wall, concentrated suspensions were observed to have non-Newtonian behavior. In this study, to determine the true rheological behavior of model concentrated suspensions, "multiple gap separation method" was applied using a parallel-disk rheometer. The model suspensions studied were polymethyl methacrylate particles having average particle sizes, in the range of 37–231 μm, in hydroxyl terminated polybutadiene. The effects of particle size and solid particle volume fraction on the wall slip and the true viscosity of model concentrated suspensions were investigated. It is observed that, as the volume fraction of particles increased, the wall slip velocity and the viscosity corrected for slip effects also increased. In addition, for model suspensions in which the solid volume fraction was ≥81% of the maximum packing fraction, non-Newtonian behavior was observed upon wall slip correction. On the other hand, as the particle size increased, the wall slip velocity was observed to increase and the true viscosity was observed to decrease. J Appl Polym Sci 98: 439–448, 2005

Key words: rheology; viscosity; particle size distribution; shear; suspension

INTRODUCTION

The rheological properties of suspensions of solid particles in polymeric matrices are important in analyzing the processing of such materials, which are encountered in several industries. The rheological behavior of these composite systems depends on the particle shape, size and size distribution, volume fraction of particles, particle–particle and particle–matrix interactions, matrix rheology, and measurement conditions such as the temperature and shear rate. Dilute suspensions of small particles in Newtonian fluids also behave as Newtonian fluids in most cases. However, despite the importance of the problem, few experimental data exist for the effects of solids concentration and particle size distribution on the rheological properties of highly concentrated suspensions. The situation for concentrated suspensions is even more difficult to analyze from a theoretical perspective compared to dilute suspensions. The methods available to tackle the problem are to introduce a technique for averaging the influence of neighboring particles or, alternatively, to simulate the situation using computer modeling.

Chong and Christiansen[1] investigated the dependency of the viscosity of highly concentrated suspensions on solid concentration and particle size distributions by using an orifice viscometer. They formulated an empirical equation that correlates the relative viscosity of suspensions as a function of solid concentration and particle size distribution of spherical particles. The determined equation reduces to the well-known Einstein equation at dilute solid concentrations.

Krieger and Dougherty[2] investigated the behavior of concentrated suspensions and obtained an empirical equation relating the concentration of solids to the viscosity of the suspensions. The Krieger–Dougherty equation is

$$\eta = \eta_s(1 - \phi/\phi_m)^{-[\eta]\phi_m} \tag{1}$$

where η_s is the suspending medium viscosity, ϕ is the filler fraction, ϕ_m is the maximum packing fraction, and $[\eta]$ is intrinsic viscosity.

Nielsen[3] developed an empirical expression to predict the concentration dependency of relative viscosity, including the particle shape factor and maximum volume fraction. According to this equation

$$\eta_r = \frac{1 + A\phi}{1 + \psi\phi} \tag{2}$$

in which $A = k_E - 1$ and

$$\psi = 1 + \left(\frac{1 - \phi_m}{\phi^2}\right)\phi$$

Correspondence to: U. Yilmazer (yilmazer@metu.edu.tr).

where k_E is the Einstein coefficient, which has the value of 2.5 for spherical particles.

According to Metzner,[4] in highly concentrated suspensions, there are two mechanisms that might lead to the importance of variations in particle size. First, during the flow of a concentrated suspension, the relative motion of particle layers might be significantly affected by modest differences in particle size. Second, and more important, major changes in the maximum possible packing density of the particles will occur with a wide distribution of particle sizes.[4] The distribution of particle sizes has little effect on suspension viscosity when the volumetric concentration of solids is <20%. At high concentration levels, the effects are of enormous magnitude. Extraordinarily high solids concentration can be achieved by using multimodal distributions of particle size.[4]

Poslinski et al.[5] studied the influence of particulate and matrix properties on the shear viscosity. As expected, shear viscosity was observed to increase with increasing solid concentration, and some of the composite systems exhibited a yield stress.

Soltani and Yilmazer[6] studied the effects of the solid content, particle size, type of solid particle material, and the temperature on the viscosity of concentrated suspensions. They observed that the viscosity of suspensions with small particles is greater than the viscosity of the suspensions with larger particles. Above 40% filler content, suspensions were observed to exhibit dilatancy. The viscosity was observed to increase with filler content and decrease with temperature.

The origins of this shear thickening behavior were explored in various investigations.[7–16] Recently, Bournonville and Nzihou[15] investigated the rheological behavior of silica-based suspensions by means of a rotational viscometer. They observed shear thinning behavior and explained this behavior with the alignment and ordering of the particles.

Olhero and Ferreira[16] observed both shear thinning and shear thickening behavior (at higher shear rates) with suspensions of fly ash. They also proposed an explanation similar to that of Bournonville and Nzihou[15] for the shear thinning behavior. They explained the shear thickening behavior at higher shear rates with the increase in the average distance between particles in the flow direction during flow. Thus, the capillary forces opposing flow cause an increase in the viscosity.

On the other hand, some have seen thickening as a result of an order–disorder transition. Hoffman[11] concluded that particles ordered in layers will shear thicken as the result of flow instability. At a certain critical shear rate, some particles will move out of their layers and disrupt the flow, resulting in an increase of the suspension viscosity.

However, in contrast to these studies, in some suspensions with coarse particles, at volume fractions of filler close to ϕ_{max}, dilatancy is not observed.[1,5,8,14] Lack of information on the important particle size distribution, particle to particle and particle to wall interactions, and the roughness of the wall do not permit a generalization for the presence or lack of dilatancy in such systems. One possible explanation is that dilatancy may not be observed if the proper corrections for slip at the wall are not carried out.[4,17]

Yilmazer and Kalyon[17] investigated some important aspects of the rheological properties of highly filled suspensions such as mat formation and flow instabilities, slip effects, and the shear-induced migration of particles. They studied various factors in the rheological characterization of highly concentrated noncolloidal suspensions that exhibit slip and found that the slip effects at the wall were very significant and the slip velocity increased with increasing shear stress at the wall. Upon slip correction, the suspension was found to exhibit dilatancy at relatively high shear stress values.

For highly concentrated suspensions, slip at the wall of the viscometer is usually a controlling factor. When the material is sheared, large velocity gradients are produced in the low-viscosity resin-rich layer near the wall. This results in "apparent slip" of the bulk fluid. The decreased concentration of particles near the wall causes an apparent slip affect, that is, the occurrence of a relative velocity between the fluid near the wall and the wall itself. For unfilled polymeric melts, the mechanism of slip is referred to as "true slip," in which case there exists a discontinuity in the velocity between the polymer and the wall.[18] The rheological data of a suspension exhibiting wall slip need to be corrected to characterize the true rheological behavior of the suspension.[18]

The use of torsional flows to determine wall slip behavior is fairly recent compared with the characterization of wall slip behavior in capillary flows. The parallel-disk geometry has several experimental advantages over other geometries, such as flow regularity and ease of sample preparation, but it has the disadvantage of nonuniform shear strain in the sample. The traditional method of correcting for wall slip and obtaining the slip velocity versus shear stress information in parallel-disk torsional flows involves experiments with multiple gap separations.[19] To determine wall slip velocity and actual shear rate in parallel-disk experiments, Yoshimura and Prud'homme[19] outlined a method based on two sets of experiments at two gap heights and a procedure for correcting the parallel-disk torsional flow data. They assumed that the wall-layer thickness is very small compared to the viscometer dimensions. They treated wall slip as a discontinuity in velocity (actual slip), where the slip velocity is defined as the difference between the velocity of the wall and that of the fluid at the wall. They

TABLE I
Specifications of PMMA Particles

Material	ϕ_m (vol %)	Average particle size (μm)	Supplier
PMMA-CMW	71.1	37.2	CMW1 Bone Cement by DePuy Int. Ltd.
PMMA-X	62.0	83.6	Meliodent by Bayer Dental
PMMA-Y	64.6	121.2	Meliodent by Bayer Dental
PMMA-HU	59.5	188.2	Synthesized by Hacettepe University–Ankara Chem. Eng. Dept. of
PMMA-Aldrich	64.2	234.6	Aldrich

also assumed that once steady state is achieved, the slip velocity is a function of stress only.

Yilmazer and Kalyon[17] generalized this method by using experiments at more than two gap heights, which provided better accuracy. Upon slip correction, the highly filled suspensions studied were found to exhibit dilatancy (shear thickening) at relatively high shear stress values.[20]

Kalyon et al.[21] characterized the rheological behavior of a very concentrated suspension (76.5 vol %) with parallel-disk and capillary viscometers. The suspension exhibited shear thinning over the apparent shear rate range of 30–3000 s^{-1}. Significant slip at the wall was observed in both torsional and capillary flows, with the slip velocity increasing sharply with increase in shear stress. A flow visualization technique was applied directly for the first time to determine the wall slip velocities in torsional flow, to also provide the true deformation rate.

Soltani and Yilmazer[18] investigated the rheological behavior of highly filled suspensions consisting of a Newtonian matrix mixed with two different sizes of aluminum powder and two different sizes of glass beads using a parallel-disk rheometer, with emphasis on the wall slip phenomenon. In these suspensions, the slip velocity was observed to increase linearly with the shear stress. At constant shear stress, the slip velocity was observed to increase with increasing temperature. The slip layer thickness was observed to increase proportionally with increasing size of the particles for glass beads up to a certain value of ϕ/ϕ_m. The slip layer thickness divided by the particle diameter δ/D_p was zero at low ϕ/ϕ_m, but it suddenly increased and reached a value that was independent of ϕ/ϕ_m and the temperature.

The aim of the present study is to investigate the effects of particle size and particle volume fraction on the wall slip of concentrated polymeric suspensions using a wider range of particle sizes than ones used in Soltani and Yilmazer.[18] Another goal is to determine the "true viscosity" of these model concentrated polymeric suspensions. This information has been lacking in the literature.

EXPERIMENTAL

Materials

The polymer matrix of the concentrated suspensions hydroxyl-terminated polybutadiene (HTPB), manufactured by ARCO (Atlantic Richfield, Los Angeles, CA), has a specific gravity of 0.786. In the shear rate range of 0.04 to 0.6 s^{-1}, the shear viscosity of HTPB was determined to be 2.4 Pa·s at 25°C, independent of the deformation rate. The suspensions were prepared with solid particles of polymethyl methacrylate (PMMA) having various average particle sizes. The specifications and the maximum volume fractions of the PMMA particles contained in the suspensions are given in Table I and the size distributions are shown in Figures 1–5. The particle size distribution analysis was done using a Mastersizer X particle size analyzer (Malvern Instruments, Malvern, UK). The specific gravity of PMMA particles at 25°C is 1.19. PMMA-X and -Y type particles were obtained by sieving original Meliodent ™, manufactured by Bayer Dental (division of Bayer AG, Leverkusen, Germany) and used in den-

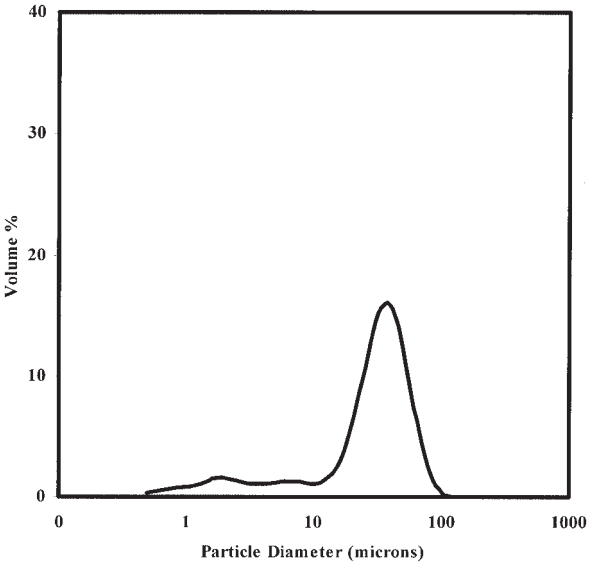

Figure 1 Particle size distribution of PMMA-CMW.

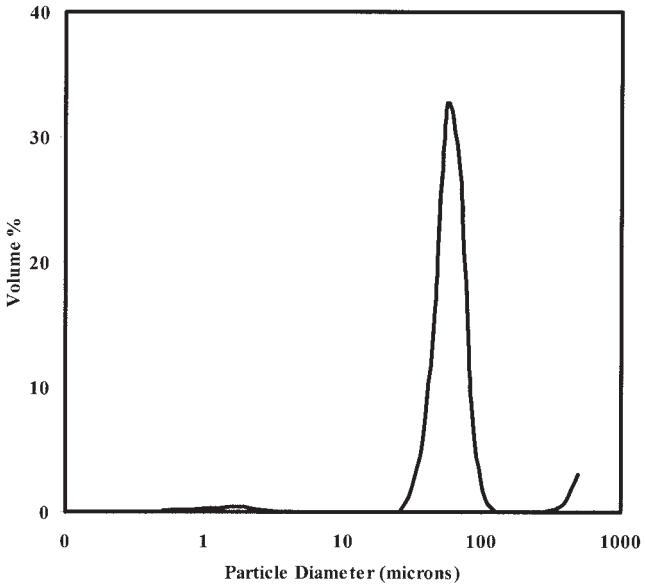

Figure 2 Particle size distribution of PMMA-X.

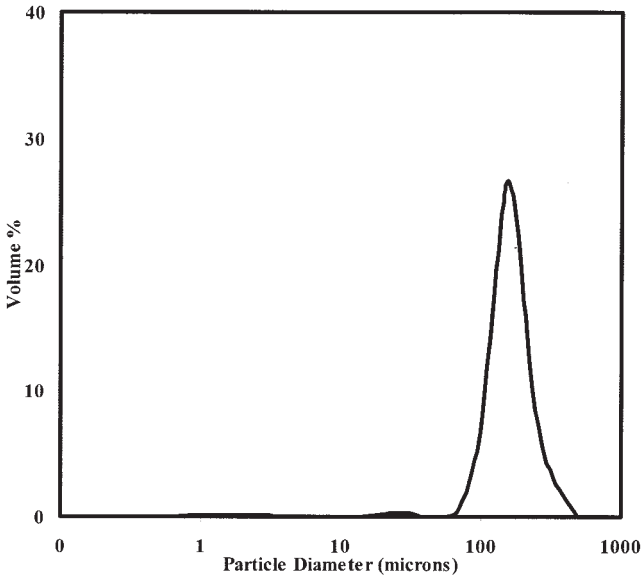

Figure 4 Particle size distribution of PMMA-HU.

tal applications. By sieving, narrower particle size distributions and two types of particles with different average particle sizes were obtained. PMMA-CMW is known as CMW1 Original Bone Cement ™, manufactured by DePuy International Ltd. (Leeds, UK). It is used as bone cement in medical applications.

Preparation of the suspension samples

The maximum packing fraction of the PMMA particles was determined by a sedimentation-in-air method. In this method, particles are poured into a container by vibration and the container is tapped at certain time intervals. Once the apparent volume is measured, the apparent density can be calculated by dividing the mass of the sample by its apparent volume. Then the maximum packing fraction can be determined by the following equation:

$$\phi_m = \frac{\varphi_{app}}{\varphi_{ac}} \tag{3}$$

where φ_{app} and φ_{ac} are apparent density and actual density of particles, respectively.

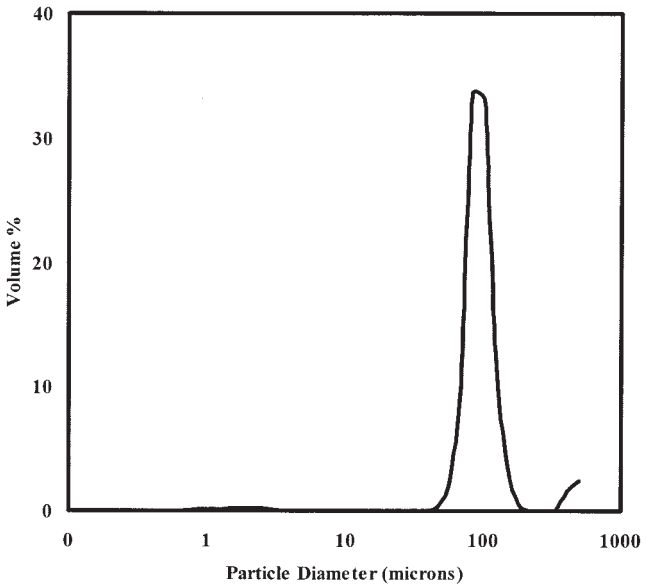

Figure 3 Particle size distribution of PMMA-Y.

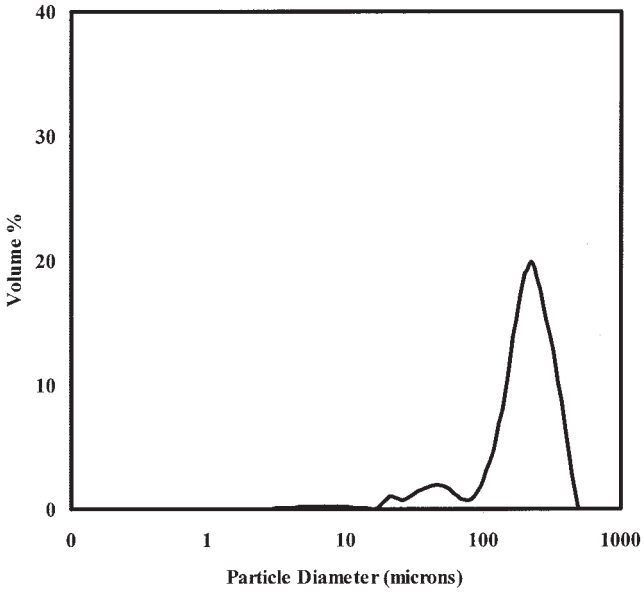

Figure 5 Particle size distribution of PMMA-Aldrich.

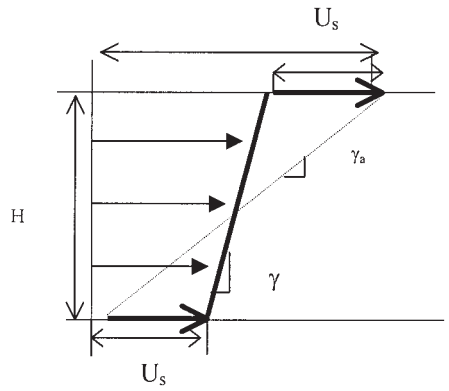

Figure 6 Parallel-disk geometry.[19]

The mixing of HTPB matrix fluid with PMMA particles was carried out for about 20 min to remove the air bubbles in the prepared suspension. The procedure used during the characterization of rheological properties is very important to achieve reproducible results.

Setup and procedure

The suspension samples were characterized by means of a parallel-disk rheometer (Haake, Bersdorff, Germany). The setup contains the Rotovisco RV20 with a CV20 measuring system that is linked to a computer. The diameters of the used disks were 19.25 mm. In the experiments, approximately 1 mL of the suspension was injected on the lower disk, and then the upper disk was brought down and the gap height was adjusted. The lower disk was rotated at a definite rotational speed by the dc drive motor, whereas the upper plate was held stationary. The resulting torque was measured in the steady-state shear mode. The torsional flow behavior of the concentrated suspensions was characterized at 25°C, using various gap heights in the range of 1 to 3 mm. Multiple gap heights were used to determine and incorporate corrections for slip at the wall.[17,19] In each experiment, a fresh sample was injected and the preshearing of the sample was avoided.

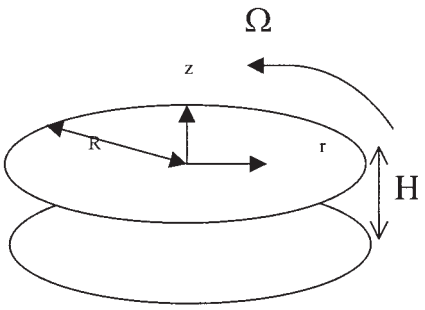

Figure 7 Parallel-disk velocity field.[19]

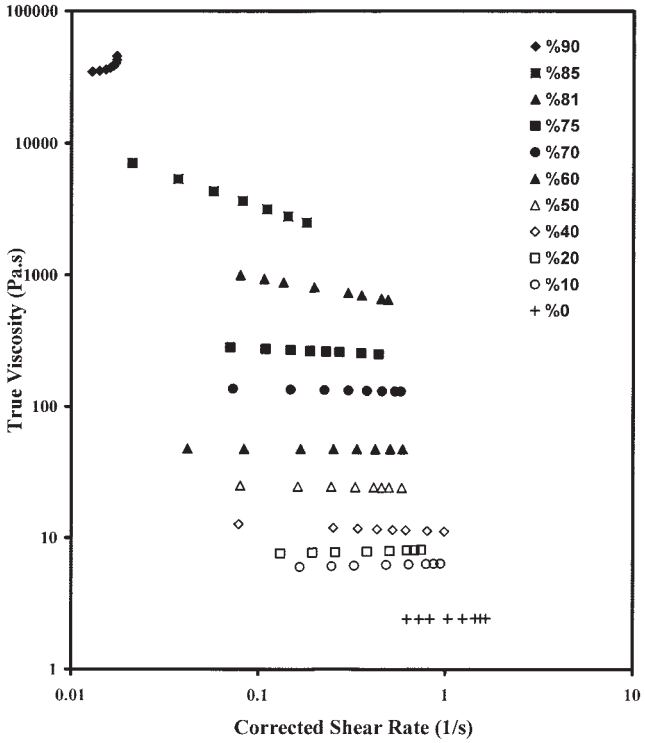

Figure 8 Effect of volume fraction of PMMA-X on viscosity for copper with surface roughness 0.65 μm.

RESULTS AND DISCUSSION

Rheological characterization

The parallel-disk geometry considered is shown in Figures 6 and 7. The upper disk is rotated at angular

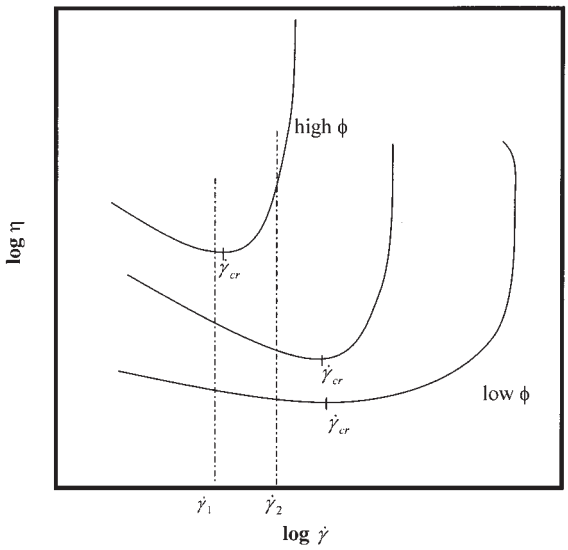

Figure 9 Schematic representation of viscosity versus shear rate for shear thickening systems, with phase volume as parameter.[22]

velocity Ω, relative to the lower disk. For narrow gap separations, the stress $\tau_{z\theta}$ is nearly constant across the gap at any particular radial position. This results in a linear velocity profile as shown in Figure 7, where the slip velocity U_s is the same at the two walls because of the equal stresses.

The velocity of the top disk is Ωr, where r is the radial distance as shown in Figure 7.[19] The slip velocity is given by[19]

$$\Omega r = H\dot{\gamma}(\tau_{z\theta}) + 2U_s(\tau_{z\theta}) \tag{4}$$

where $\dot{\gamma}$ is the shear rate experienced by the fluid and H is the gap height.

In parallel-disk torsional flow, the apparent shear rate $\dot{\gamma}_a$ (not corrected for slip effects) is a linear function of the radius r, given by

$$\dot{\gamma}_a = \frac{\Omega r}{H} \tag{5}$$

At the edge of the disk, the apparent shear rate can be found from eq. (6) obtained from eq. (5) by substituting $r = R$. Thus,

$$\dot{\gamma}_{aR} = \frac{\Omega R}{H} \tag{6}$$

The apparent shear rate $\dot{\gamma}_a$ can be related to the true shear rate $\dot{\gamma}$, and slip velocity U_s, by dividing eq. (4) by H and substituting eqs. (5) and (6) in eq. (4):

$$\dot{\gamma}_a = \dot{\gamma}(\tau_{z\theta}) + \frac{2U_s(\tau_{z\theta})}{H} \tag{7}$$

The torque T required to rotate the upper disk is given by

$$T = 2\pi\int_0^R r^2\tau_{z\theta}dr \tag{8}$$

Through eq. (5), one can arrange the variable of integration from r to $\dot{\gamma}_a$ to obtain

$$T = \frac{2\pi R^3}{\dot{\gamma}_{aR}^3}\int_0^{\dot{\gamma}_{aR}} \dot{\gamma}_a^2\tau_{z\theta}(\dot{\gamma}_a)d\dot{\gamma}_a \tag{9}$$

Then, by differentiating eq. (9) with respect to $\dot{\gamma}_{aR}$ the corrected shear stress at the edge of the disk τ_R is obtained as

$$\tau_R = \frac{T}{2\pi R^3}\left(3 + \frac{d\ln T}{d\ln\dot{\gamma}_{aR}}\right) \tag{10}$$

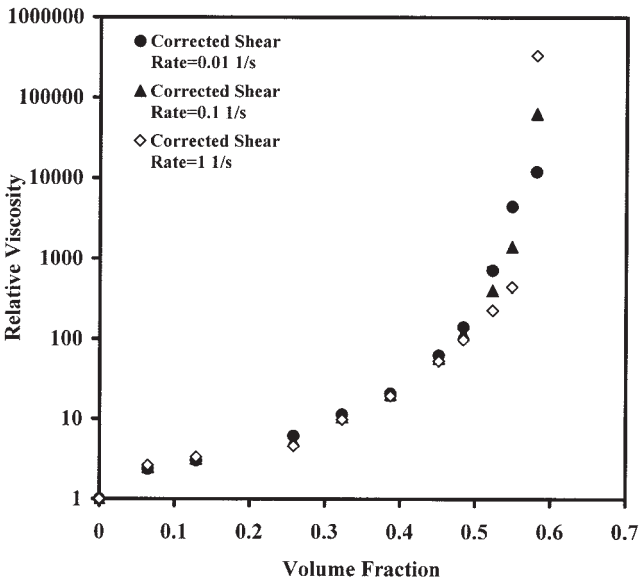

Figure 10 Relative viscosity versus volume fraction for various shear rate values using PMMA-X.

This step is analogous to the differentiation that produces the Weissenberg–Rabinowitch equation for flow in a capillary. The function $f = (d\ln T)/(d\ln\dot{\gamma}_{aR})$ is dependent on the gap height used. Note that, for a Newtonian material, the shear stress is given by $\tau_R = 2T/\pi R^3$ because the second term in parentheses is equal to one.

Equation (7) also applies at $r = R$; thus, it can be written as

$$\dot{\gamma}_{aR} = \dot{\gamma}_R(\tau_R) + \frac{2U_s(\tau_R)}{H} \tag{11}$$

If plots of $\dot{\gamma}_{aR}$ versus $1/H$ are drawn at constant τ_R, then straight lines are obtained according to eq. (11). The extrapolated intercepts are equal to $\dot{\gamma}_R(\tau_R)$ (i.e., the true shear rate at the edge), and the slopes are equal to $2U_s(\tau_R)$.

The true viscosity η_s can then be calculated by dividing the shear stress at the edge of the disk by the true shear rate at the edge of the disk:

$$\eta_s = \frac{\tau_R}{\dot{\gamma}_R} \tag{12}$$

The slip velocity values in parallel-disk torsional flow experiments are calculated using the slopes as implied by eq. (11). In most cases, the graphs of slip velocity versus τ_R behavior follow a power-law relationship such as

$$U_s = a\tau_R^m \tag{13}$$

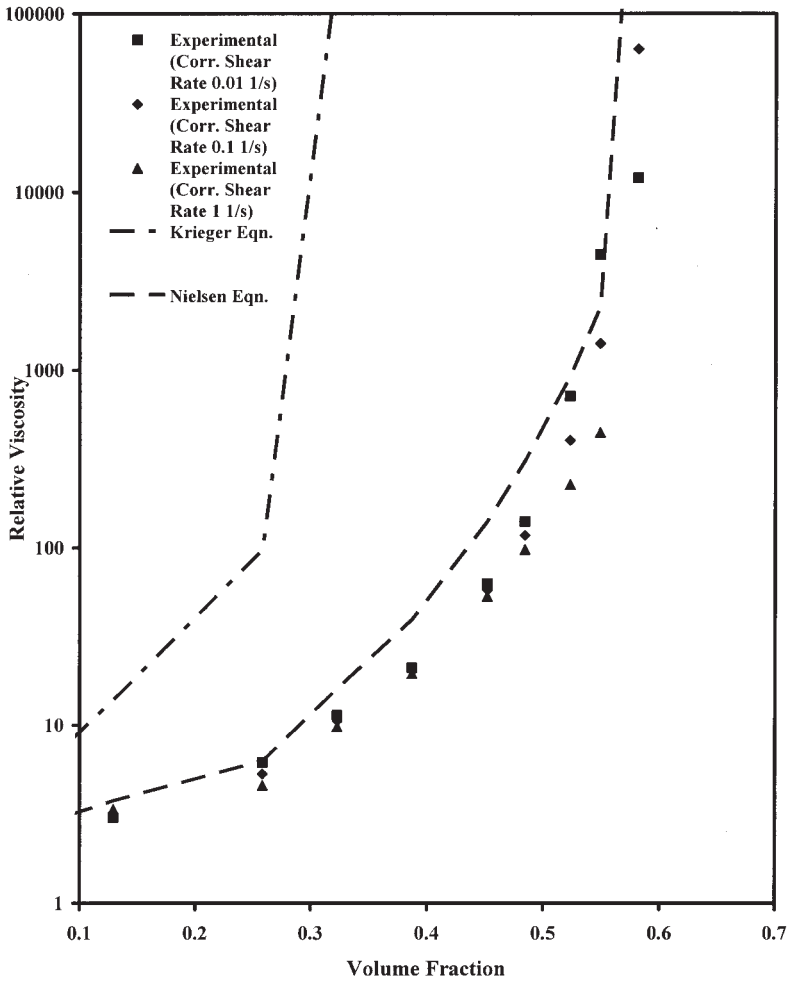

Figure 11 Comparison of existing viscosity models in the literature with the experimental values using PMMA-X.

Effect of volume fraction of particles on slip at the wall and the shear viscosity

In this part, the behavior of PMMA-X–type filler on copper with 0.65 μm surface roughness is reported. Figure 8 shows that the viscosity calculated from eq. (12) increases with increasing volume fraction, from 0 through 90% of the maximum packing fraction of particles. The increase in viscosity for the highly filled suspensions is observed to be three to four orders of magnitude. For volume fractions, which are lower than 81% of the maximum packing fraction, suspensions show Newtonian behavior.

In suspensions containing fillers equal to 81 and 85% of the maximum packing fraction, viscosity decreases with increasing shear rate, exhibiting shear-thinning behavior. This behavior is observed to be more significant for 85% of the maximum packing fraction.

On the other hand, for 90% of the maximum packing fraction, viscosity is found to increase with increasing shear rate, exhibiting shear thickening or dilatancy. At this volume fraction, although the apparent shear rate range was the same as that used for other volume fractions, the corrected shear rate values are observed to be much lower than those at lower volume fractions as a result of more significant wall slip effects.

The shear thinning observed at low volume fractions of particles and the shear thickening observed at high volume fractions can be understood from Figure 9, which describes the rheological behavior of concentrated suspensions.[22]

Concentrated suspensions exhibit shear thinning at low shear rates and shear thickening at high shear rates. Basically, at low shear rates the particles may easily slide over each other and exhibit shear thinning, whereas at high shear rates the particle–particle interactions are higher and particles cannot slide over each other, resulting in shear thickening. There is a critical shear rate $\dot{\gamma}_{cr}$, above which shear thickening starts. However, $\dot{\gamma}_{cr}$ is a function of filler content and particle size. It is lower for a high volume fraction of particles, as seen from Figure 9. Thus, one may observe shear thickening at high volume fractions and shear thin-

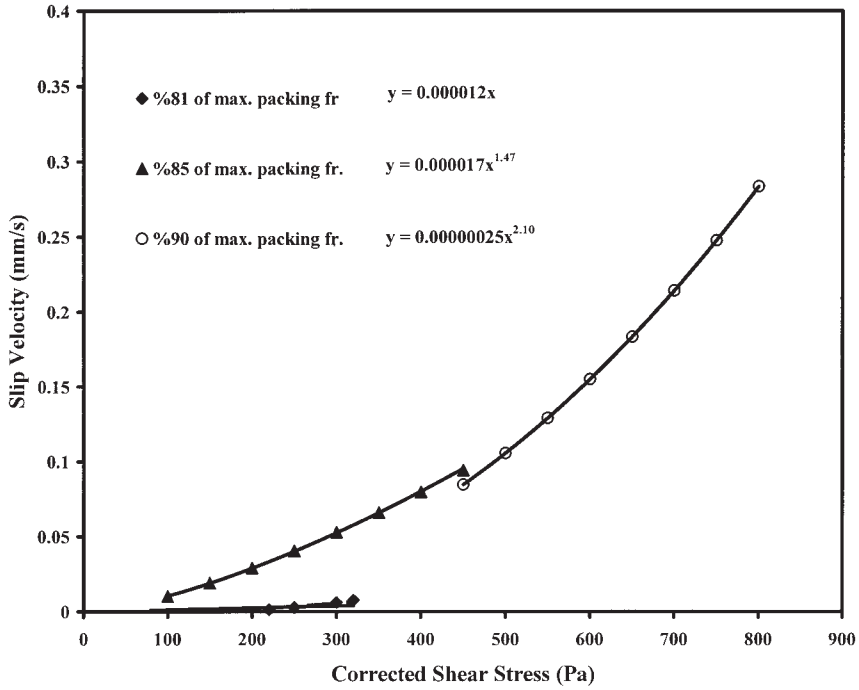

Figure 12 Effect of volume fraction on slip velocity for copper with surface roughness 0.65 μm using PMMA-X.

ning at lower volume fractions in the region of the shear rates from $\dot{\gamma}_1$ to $\dot{\gamma}_2$.

The interparticle distance H can be calculated from eq. (14) given by Chander[23] as

$$H = D[(\phi_m/\phi)^{1/3} - 1] \tag{14}$$

in which D is the diameter of the spheres.

Using the data presented here, it is observed that when H/D is >0.3 the suspensions are Newtonian. However, if H/D decreases to a value between 0.15 and 0.30, then shear-thinning takes place. If H/D is <0.15, shear thickening behavior is encountered.

An explanation for the non-Newtonian behavior of the concentrated suspensions could be given according to Olhero and Ferreira,[16] who stated that concentrated suspensions show shear thinning behavior as a result of the decrease in their viscosity, caused by the alignment and the ordering of the particles at low shear rates. However, at high shear rates the interparticle spacing in the flow direction increases as a result of flow. Thus, the capillary forces opposing the flow cause an increase in the viscosity, resulting in shear thickening.

One can see from Figure 10 that the relative viscosity determined for the suspensions studied in this report depends on the shear rate. This shear rate dependency is observed to be more significant at 81, 85, and 90% of the maximum packing fractions arising from the shear thickening and/or shear thinning behavior explained earlier. Thus, to formulate a better viscosity model for the viscosity of concentrated suspensions, one must take into account the slip at the wall and the shear rate effect.

Comparing the experimental data obtained in this study with the existing viscosity models, it can be seen from Figure 11 that Nielsen's model is found to be the most suitable model for the experimental values observed here, although the determined maximum packing fraction ($\phi_m = 0.646$) is higher in our experiments than that determined using the assumption of Nielsen ($\phi_m = 0.601$–0.637).

On the other hand, slip velocity versus corrected shear stress graphs at 81, 85, and 90% of maximum packing fractions are shown in Figure 12. As the volume fraction increases, the m values in eq. (13) also increase, although a values are observed to abruptly decrease at 90% of the maximum packing fraction.

However, the slip velocity values are found to be very close to each other at 85 and 90% of maximum volume fractions at a shear stress of approximately 450 Pa. Another observation is that the slip velocity values are approximately zero at 81% of maximum volume fraction, indicating that at lower volume fractions, the slip velocities could be insignificant.

Effects of particle size on slip at the wall and the shear viscosity

To investigate the effect of particle size on viscosity and wall slip velocity, copper disks with surface roughness of 0.65 μm were used and the volume

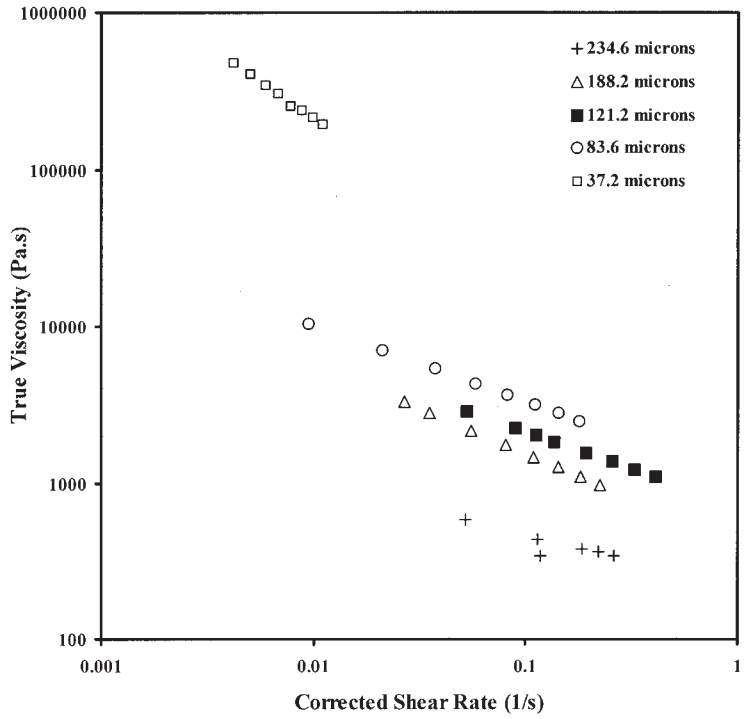

Figure 13 Effect of particle size on true viscosity on copper with surface roughness 0.65 μm.

fraction was kept constant at 85% of the maximum volume fraction during the experiments.

As seen from Figure 13, as the average particle size increases, the "true" viscosity values are observed to decrease. Moreover, shear-thinning behavior is observed for all the particle sizes studied. The factors for obtaining shear-thinning behavior are unaffected by the average particle size of the

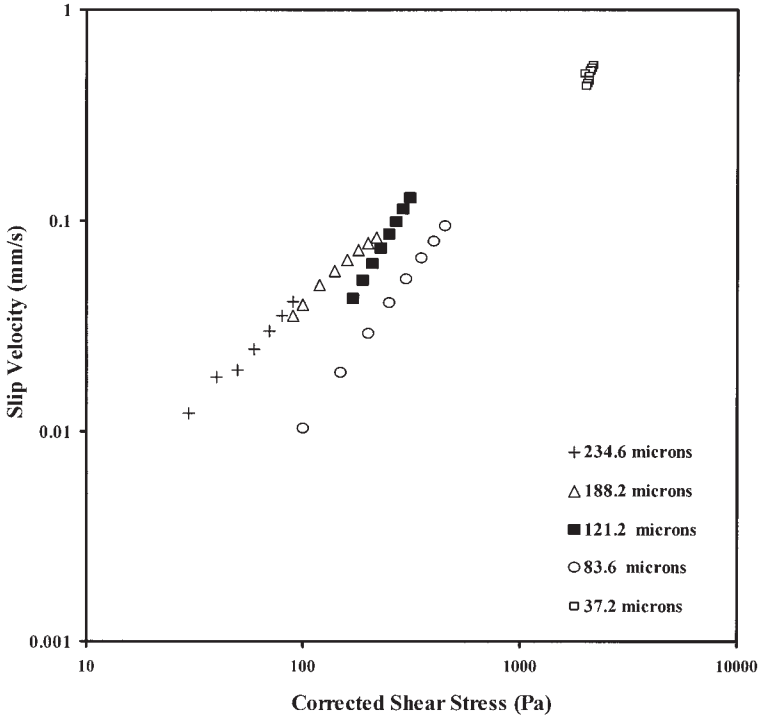

Figure 14 Effect of particle size on slip velocity on copper with surface roughness 0.65 μm.

fillers in the size range studied, the polymer matrix, and test conditions.

The shear-thinning behavior of the suspensions is also independent of the slightly changing particle size distribution of the PMMA particles at different particle sizes. The reason for the change in slopes in Figure 13 could be the slight difference in the particle size distribution of particles.

On the other hand, the slip velocity values are observed to decrease with decreasing average particle size of the fillers. At constant shear stress, this behavior can be seen from Figure 14. The reason for this behavior is the steric hindrance effect of the particles. That is, as the particle size increases, the particles cannot approach very close to the wall and this causes the slip layer thickness to increase. As a result, the slip velocity is observed to increase.

CONCLUSIONS

The effects of particle size and volume fraction on the wall slip and viscosity of the concentrated suspensions of PMMA (polymethyl methacrylate) particles in HTPB (hydroxyl-terminated polybutadiene) were investigated. The main conclusions of the study are as follows:

1. For volume fractions that are lower than 81% of the maximum packing fraction, the model suspensions show Newtonian behavior. For volume fractions between 81 and 90% of the maximum packing fraction, the model suspensions show shear-thinning behavior. On the other hand, at 90% of the maximum packing fraction, the model suspensions exhibit shear thinning followed by shear-thickening behavior.
2. As the volume fraction of particles in the suspension increases, the wall slip velocity increases. At low volume fractions of particles, the wall slip could be insignificant.
3. As the particle size increases, the wall slip velocity also increases as the result of the steric hindrance effect.

References

1. Chong, J. S.; Christiansen, E. B. J Appl Polym Sci 1971, 15, 2007.
2. Krieger, I. M.; Dougherty, J. J. Trans Soc Rheol 1959, 3, 137.
3. Nielsen, L. E. Polymer Rheology; Marcel Dekker: New York, 1977; Chapter 7.
4. Metzner, A. B. J Rheol 1985, 29, 739.
5. Poslinksi, A. J.; Ryan, M. E.; Gupta, R. K.; Seshadri, S. G.; Frechette, F. J. J Rheol 1988, 32, 703.
6. Soltani, F.; Yilmazer, U. Adv Polym Technol 1999, 18, 336.
7. Frith, W. J.; Lips, A. Adv Colloid Interface Sci 1995, 61, 161.
8. Metzner, A. B.; Whitlock, M. 1958, 2, 239.
9. Green, R. G.; Griskey, R. G. Trans Soc Rheol 1968, 12, 13.
10. Green, R. G.; Griskey, R. G. Trans Soc Rheol 1968, 12, 27.
11. Hoffman, R. L. Trans Soc Rheol 1972, 16, 155.
12. Strivens, T. A. J Colloid Interface Sci 1976, 57, 476.
13. Marrucci, G.; Denn, M. M. Rheol Acta 1985, 24, 317.
14. Tsai, S. C.; Zammoouri, K. J Rheol 1988, 32, 737.
15. Bournonville, B.; Nzihou, A. Powder Technol 2002, 128, 148.
16. Olhero, S. M.; Ferreira, J. M. F. Powder Technol 2004, 139, 69.
17. Yilmazer, U.; Kalyon, D. M. J Rheol 1989, 33, 1197.
18. Soltani, F.; Yilmazer, U. J Appl Polym Sci 1998, 70, 515.
19. Yoshimura, A. S.; Prud'homme, R. K. J Rheol 1988, 32, 53.
20. Yilmazer, U.; Kalyon, D. M. ANTEC 1989, 89, 1682.
21. Kalyon, D. M.; Yaras, P.; Aral, B. K.; Yilmazer, U. J Rheol 1993, 37, 35.
22. Barnes, H. A.; Hutton, J. F.; Walters, K. An Introduction to Rheology; Elsevier: Amsterdam, 1989.
23. Chander, A. Colloid Surf A Physicochem Eng Aspects 1998, 133, 143.